

Data Acquisition

24. Data Acquisition by Imaging Detectors

Imaging sensors convert radiative energy into an electrical signal and such sensors are available that cover the wide spectrum from gamma rays to the infrared. They accumulate an electrical signal during the exposure time and convert all the signals of an array of detectors into a time-serial analog or digital data stream. The dominate and most successful devices to perform this task are charge coupled devices (CCD). However directly addressable imaging sensors on the basis of CMOS fabrication technology are becoming more and more promising because the image acquisition, digitalization and preprocessing can be integrated on a single chip; hence yielding very fast frame rates. This chapter provides a comprehensive survey of the available imaging sensors, details the parameters that control their performance and gives practical tips to select the best camera for different imaging tasks.

24.1	Definitions	1419
24.2	Types of Detectors	1420
24.2.1	Quantum Detectors	1420
24.2.2	Thermal Detectors	1420
24.3	Imaging Detectors	1421
24.3.1	The Charge-Coupled Device	1421

24.1 Definitions

An imaging sensor converts an *image*, i. e., the spatially varying irradiance projected on the image plane by an optical system into a digital data stream that can be stored and processed by a digital computer. This involves a number of steps Fig. 24.1:

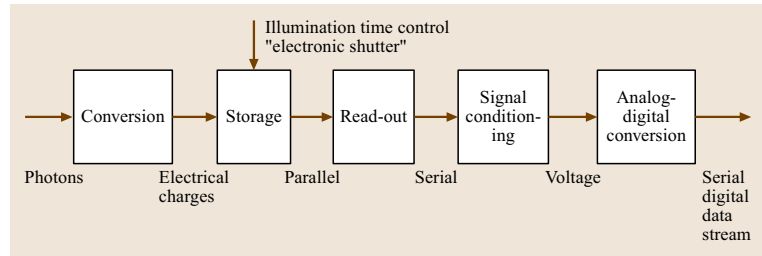
- **Conversion.** The incident radiative energy is converted into an electrical charge, voltage, or current. In order to form an image, an array of detectors is required. Each of the detector elements integrates the incident irradiance over a certain area.
- **Storage.** The generated charges must be integrated and thus stored over a certain time interval, the *exposure time*.

24.3.2	CMOS Imaging Sensors	1421
24.3.3	CCD Sensor Architectures	1422
24.3.4	Standard Interfaces for Digital Cameras	1425
24.4	Performance of Imaging Sensors	1426
24.4.1	Responsivity	1426
24.4.2	Quantum Efficiency	1426
24.4.3	Signal Irradiance Relation	1427
24.4.4	Dark Current	1427
24.4.5	Noise-Equivalent Exposure	1427
24.4.6	Saturation Equivalent Exposure ...	1427
24.4.7	Dynamic Range	1428
24.4.8	Photon-Noise-Limited Performance	1428
24.4.9	Linear Noise Model for Image Sensors	1429
24.4.10	Signal-to-Noise Ratio	1429
24.4.11	Spectral Sensitivity	1431
24.4.12	Nonuniform Responsivity	1433
24.4.13	Artifacts and Operation Errors	1433
24.5	Camera Selection	1435
24.5.1	Measurements at Low Light Levels	1435
24.5.2	Measurements with High Irradiance Variations ...	1435
24.5.3	Precise Radiometric and Geometric Measurements	1435
References	1436

sure time. In order to control illumination, the sensor should accumulate charges only during a time interval that can be controlled by an external signal. This feature is called an *electronic shutter*.

- **Read-out.** The exposure, the accumulated electrical charges must be read out. This step essentially converts the spatial charge distribution (parallel data) into one (or multiple) sequential data stream that is then processed by one (or multiple) output circuit.
- **Signal conditioning.** In a suitable electrical amplifier, the read-out charge is converted into a voltage

Fig. 24.1 Chain of processes that takes place in an imaging sensor that converts incident photons into a serial digital data stream



and by appropriate signal conditioning reduced from distortions. In this stage, also the responsivity of the sensor can be controlled.

- **Analog–digital conversion** In a final step, the analog voltage is converted it into a digital number for input into a computer.

24.2 Types of Detectors

For imaging detectors, basically two types of detectors are utilized: quantum detectors and thermal detectors.

24.2.1 Quantum Detectors

The term *quantum detector* refers to a class of detectors where the absorption of the smallest energy unit for electromagnetic radiation, the *photon*, triggers the detection of radiation. This process causes the transition of an electron into a higher excited state. Three variants are possible, which lead to three subclasses of quantum detectors.

Photoemissive Detectors

By the absorption of the photon, the electron receives enough energy to be able to leave the detector and become a *free electron*. This effect is known as the (extrinsic) *photo effect*. The photo effect can be triggered only by photons below a critical wavelength (i. e., above a certain energy of the photon that is sufficient to provide enough energy to free the electron from its binding).

Photoemission of electrons is utilized in *vacuum photo tubes* and *photomultiplier tubes (PMT)*. PMTs are sensitive enough to count single photons, since the initial electrons generated by photon absorption are accelerated to hit another dynode with sufficient energy to cause the ejection of multiple secondary electrons. This process can be cascaded to achieve high gain factors. Because PMTs have short response times that may be less than 10^{-10} s, individual photons can be counted as short current impulses. Such a device is known as a *photon-counting device*.

Radiation detectors based on the photo effect can be sensitive only in a quite narrow spectral range. The lowest wavelength is given by the minimum energy required to free an electron. For higher photon energies, the material may become more transparent, leading to a lower probability that the photon is absorbed.

Photovoltaic and Photoconductive Detectors

Semiconductor devices that utilize the inner photo effect have largely replaced imaging detectors based on photoemission. A thorough understanding of these devices requires knowledge of condensed matter physics. Thus, discussion of these devices here is superficial and concentrates on the basic properties directly related to imaging detectors. The semiconductor devices have in common with the photoemissive detectors that they have a threshold energy and thus a minimum frequency of radiation is required. This is due to the fact that electrons must be excited from the valence band across a band gap to the conduction band. In the valence band, the electrons cannot move and thus cause no further effects.

In a suitable photodetector material, the conduction band is empty. The absorption of a photon excites an electron into the conduction band, where it can move rather unrestricted, thus increasing the conductance of the detector material. Detectors operating in this mode are called *photoconductive detectors*.

In an appropriately designed detector, the generation of an electron builds up an electric tension. Under the influence of this tension, an electric current can be measured that is proportional to the rate with which the

absorbed photons generate electrons. Detectors of this type are known as *photovoltaic detectors*.

24.2.2 Thermal Detectors

Thermal detectors respond to the temperature increase resulting from the absorption of incident radiation. The delivered signal is proportional to the temperature increase. The common feature of thermal detectors is the wide spectral range to which they can be made sensitive. They do not, however, reach the sensitivities of quantum detectors, since the radiation detection is based on secondary effects. The three most widely used secondary effects for imaging detectors are thermoelectricity, pyroelectricity, and thermoconductivity.

Thermoelectric Effect

Two separate junctions of two dissimilar metals at different temperatures generate a voltage proportional to the temperature difference between them. One junction must be kept at a reference temperature, while

the other be designed to absorb the electromagnetic radiation with minimum thermal mass and good thermal insulation. Such a device is known as a *thermopile*.

Pyroelectric Effect

Pyroelectric materials have a permanent electrical polarization. Changes in the temperature cause a change in the surface charges. Pyroelectric detectors can only detect changes in the incident radiant flux and thus require a chopper. Furthermore, they lose their pyroelectric behavior above a critical temperature, the Curie temperature.

Thermoconductive Effect

Some materials feature large changes in electric conductivity with temperature. A device measuring radiation by change in conductance is called a *bolometer*. Recently, microbolometer arrays have been manufactured for uncooled infrared imagers in the 8–14 μm wavelength range that show a noise equivalent temperature difference ($\text{NE}\Delta T$) of about 100 mK [24.1].

24.3 Imaging Detectors

The photovoltaic effects are most suitable for imaging detectors. Instead of moving the photoinduced electrons through the conduction band, they can be captured by additional potential walls in cells. In these cells, the electrons can be accumulated for a certain time.

Given this basic structure of a quantum detector, it is obvious that the most difficult problem of an imaging device is the conversion of the spatial arrangement of the accumulated charges into an electric signal. This process is referred to as *read-out*.

24.3.1 The Charge-Coupled Device

The invention of the *charge-coupled device (CCD)* in the mid 1970s was a breakthrough for semiconductor imaging devices. A CCD is effectively an analog shift register.

By an appropriate sequential change of potential, charge can be moved across the imaging sensor. A so-called four-phase CCD is shown in Fig. 24.2. Potential walls separate the charge packets. First, a potential wall to the left of the three-cell-wide charge-storage area is raised, confining the charges to two cells. Subsequently, a potential barrier to the right is lowered so that the

charge packets move to the right by one cell. Repeating this procedure, the charge packets can be moved all the way across the array. The charge transfer process can be made efficient enough that only a negligible fraction of electrons are *lost* during the whole transfer. The charge transfer mechanism is the base for one- and two-dimensional arrays of photosensors.

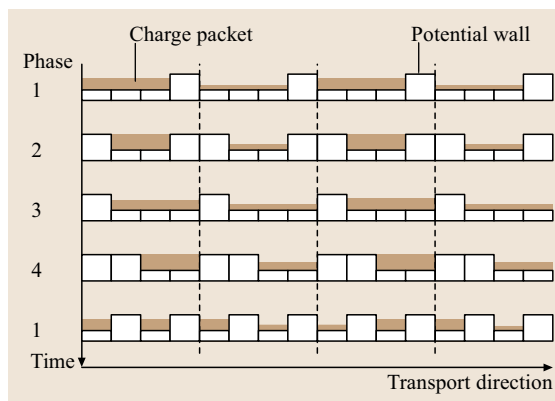


Fig. 24.2 Principle of the charge-transfer mechanisms of the charge-coupled device (CCD)

Table 24.1 Spectral sensitivity of different **CCD** sensors or focal plane areas. The last column lists either the quantum efficiency or the number of electrons generated per keV for X-ray detectors

Sensor type	Spectral range	Typical sensitivity
Scintillator, glass-fiber coupled to Si- CCD	20–100 keV	0.5 e/keV
Fiber-coupled X-ray-sensitive fluorescence coating on Si- CCD	3–40 keV	5 e/keV
Direct detection with beryllium window on Si- CCD	3–15 keV	0.3 e/keV
Specially treated, thinned, back-illuminated Si- CCD	<30 nm 30 eV–8 keV	
Si- CCD with UV fluorescence coating and MgF ₂ window	0.12–1.0 μm	< 0.4
Thinned, back-illuminated Si- CCD	0.25–1.0 μm	< 0.80
Standard silicon CCD or CMOS sensor	0.35–1.0 μm	0.1–0.65
GaAs focal plane array	0.9–1.7 μm	
Pt:Si focal plane array	1.4–5.0 μm	0.001–0.01
InSb focal plane array	1.0–5.5 μm	< 0.85
HgCdTe (MCT) focal plane array	2.5–5.0 or 8.0–12.0 μm (tunable)	
GaAs/AlGaAs quantum well photodetectors (QWIP)	3.0–5.0 or 8.0–10.0 μm (tunable)	Low
Antimonide superlattice (SL)	3.0–10.0 μm (tunable)	

24.3.2 CMOS Imaging Sensors

Active Pixel Sensors

Despite the success of **CCD** imaging sensors, there are valuable alternatives [24.2]. With the rapidly decreasing sizes of transistors on semiconductors, it is also possible to give each pixel its own preamplifier and possibly additional circuits. Such a pixel is known as an *active pixel sensor (APS)*. In this case transfer of the accumulated photocharge is no longer required. The voltage generated by the circuits of the APS is just sensed by appropriate selection circuits. In contrast to a **CCD** sensor, it is possible to read out an arbitrary part of the sensor without any speed loss and with the same pixel clock rate.

APS technology is very attractive because the imaging sensors can be produced in standard complementary metal oxide semiconductor (**CMOS**) technology and ad-

ditional analog and digital circuits can be integrated onto the chip. This opens the way to integrate the complete functionality of a camera on a single chip including analog-to-digital converters.

High-Speed CMOS Sensors

CMOS sensors offer the significant advantage that massively parallel read-out circuits can easily be added to the sensor. Therefore high-speed cameras are dominated today by **CMOS** sensors Table 24.1. The frame rates for high-speed sensors are not limited by the **CMOS** technology itself but rather by the transfer of the digital image data (Sect. 24.3.4).

24.3.3 CCD Sensor Architectures

Frame Transfer

Frame-transfer **CCD** sensors (Fig. 24.3) use the photo accumulation sites also as charge transfer registers. At the end of the exposure time, the whole frame is transferred across the whole illuminated area into an optically isolated frame storage area, where it is read out row by row with another horizontal shift register, while in the meantime the next exposure takes place in the illuminated frame array. During the transfer phase, the sensor must not be illuminated. Therefore illumination with either a flashlight or a mechanical shutter is required. The required dark period is rather short compared to the read-out time for the whole area because it is approximately equal to the time required to read out just one row.

For large-area **CCD** sensors, the extra storage area for the frame transfer can no longer be afforded. Then,

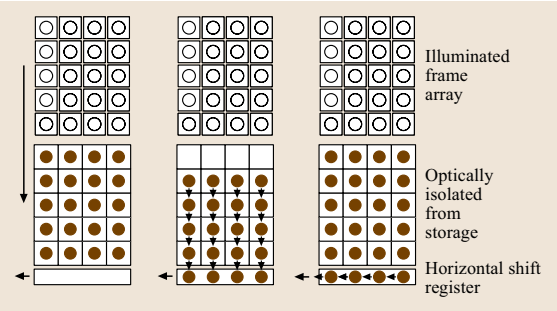


Fig. 24.3 Frame integration with a frame-transfer **CCD** sensor

Table 24.2 Selection of monochrome **CCD** imaging sensors, C: charge saturation capacity in electrons, **eNIR**: enhanced **NIR** sensitivity, FR: frame rate in s^{-1} , ID: image diagonal in mm, QE: peak quantum efficiency, Sony (ICX...) and Kodak (KAI...) sensors

Chip	Format $H \times V$	FR	ID	Pixel size $H \times V (\mu\text{m})$	Comments
Interlaced American video (EIA standard)					
ICX278AL 1/4"	768 × 494	30	4.56	4.75 × 5.55	eNIR
ICX258AL 1/3"	768 × 494	30	6.09	6.35 × 7.4	eNIR
ICX248AL 1/2"	768 × 494	30	8.07	8.4 × 9.8	eNIR
ICX422AL 2/3"	768 × 494	30	11.1	11.6 × 13.5	
Interlaced European video (CCIR standard)					
ICX279AL 1/4"	752 × 582	25	4.54	4.85 × 4.65	eNIR
ICX259AL 1/3"	752 × 582	25	6.09	6.5 × 6.25	eNIR
ICX249AL 1/2"	752 × 582	25	8.07	8.6 × 8.3	eNIR
ICX423AL 2/3"	752 × 582	25	10.9	11.6 × 11.2	
Progressive scanning interline					
ICX098AL 1/4"	659 × 494	30	4.61	5.6 × 5.6	
ICX424AL 1/3"	659 × 494	30	6.09	7.4 × 7.4	
ICX074AL 1/2" ^a	659 × 494	40	8.15	9.9 × 9.9	C 32k, QE 0.43 at 340 nm
ICX414AL 1/2"	659 × 494	50	8.15	9.9 × 9.9	C 30k, QE 0.40 at 500 nm
ICX075AL 1/2"	782 × 582	30	8.09	8.3 × 8.3	
ICX204AL 1/3"	1024 × 768	15	5.95	4.65 × 4.65	
ICX205AL 1/2"	1360 × 1024	9.5	7.72	4.65 × 4.65	C 13k
ICX285AL 2/3"	1360 × 1024	10	11.0	6.45 × 6.45	C 18k, QE 0.65 at 500 nm
ICX085AL 2/3" ^a	1300 × 1030	12.5	11.1	6.7 × 6.7	C 20k, QE 0.54 at 380 nm
ICX274AL 1/1.8"	1628 × 1236	12	8.99	4.4 × 4.4	
ICX625ALA 2/3"	2456 × 2058	15	11.0	3.45 × 3.45	
KAI-0340DM 1/3"	640 × 480	200	5.92	7.4 × 7.4	C 20k, QE 0.55 at 500 nm
KAI-1010M	1008 × 1018	30	12.9	9.0 × 9.0	QE 0.37 at 500 nm
KAI-1020M	1000 × 1000	49	10.5	7.4 × 7.4	C 42k, QE 0.45 at 490 nm
KAI-2001M	1600 × 1200	30	14.8	7.4 × 7.4	C 40k, QE 0.55 at 480 nm
KAI-4020M	2048 × 2048	15	21.4	7.4 × 7.4	C 40k, QE 0.55 at 480 nm
KAI-11002M	4008 × 2672	3	43.3	9.0 × 9.0	C 60k, QE 0.50 at 500 nm
KAI-16000M	4872 × 3248	3	43.3	7.4 × 7.4	C 30k
Electron-multiplying frame-transfer CCD					
E2V CCD97-00fi	512 × 512	40	11.6	16.0 × 16.0	C 130k, QE 0.46 at 720 nm
E2V CCD97-00bi	512 × 512	40	11.6	16.0 × 16.0	C 130k, QE 0.92 at 570 nm, thinned and back illuminated
TI TC285SPD-30	1004 × 1002	13	11.3	8.0 × 8.0	C 70k, QE 0.60 at 680 nm
In situ storage high-speed image sensors (ISIS)					
Shimadzu IS- CCD	312 × 260	10 ⁶	26.9	66.3 × 66.3	C 25k, stores up to 100 frames on chip, 13% fill factor for photogate

^a no longer available. Sources: <http://www.framos.de>, <http://www.kodak.com/global/en/digital/ccd/>, <http://www.pco.de>, <http://www.e2v.com>, <http://www.schimadzu.com>, and [24.3]

the frame is directly read out. This variant of frame-transfer sensors is called a *full-frame transfer* sensor. It has the disadvantage that the chip must not be illu-

minated during the whole read-out phase. This means that the exposure time and the read out time must not overlap. Most scientific-grade **CCD** sensors and those

used in consumer and professional digital cameras are full-frame transfer sensors.

Interline Transfer

Because frame-transfer sensors are not suitable for continuous illumination and high frame rates, the most common scan mode is the more complex *interline transfer*. Such a sensor has charge storage sites between the lines of photosensors. At the end of an exposure period, the charges collected at the photosensors are transferred to these storage sites. Then a two-stage transfer chain follows. First, the charge packets are shifted down the vertical interline storage registers. The charge package in the lowest cell of the vertical shift register is then transferred to a horizontal shift register at the lower end of the **CCD** chip, where a second transfer of an image row is shifted out to a charge-sensitive amplifier to form a time-serial analog video signal.

Electronic Shutter

A very useful feature is the *electronic shutter*. With electronic shuttering, the exposure time can be limited to shorter times than a field or frame duration. This is achieved by draining the accumulating charges at the beginning of the exposure time. Accumulation (and thus the exposure) starts when the draining is stopped and lasts until the end of the normal exposure time. Electronic shutter times can be as short as a few μs .

High Speed with In Situ Storage

At the current state of the art, the serial read-out speed of **CCD** sensors is limited to several 10 MHz. Even with up to four output taps, maximal pixel rates are only about 100 MPixel/s. A 1024×1024 sensor with 1000 frames/s, however, would require 1000 MPixel/s.

This principle limitation can be overcome if multiple charge storages are integrated for each sensor element on the chip. The price to be paid is a rather short image sequence and a small fill factor for the photosensitive area. Recently a 312×260 IS-**CCD** sensor has been introduced that can capture 100 consecutive images at 1 000 000 frames/s ([24.3], Table 24.2). This chip has large pixels ($66\text{--}66\ \mu\text{m}^2$) with a fill factor of 13% and a maximum effective pixel transfer rate into the on-chip charge storage of 80 000 MPixel/s.

Microlens Arrays

Interline transfer sensors have the disadvantage that only a rather small fraction, typically 20–30%, of the sen-

sor element is light sensitive because the main area of the sensor is required for the interline storage areas and other circuits. Arrays of microlenses can overcome this disadvantage. With such an area, each photosensor is covered by a microlens, effectively enlarging the light-collecting area and thus sensitivity by a factor of 2–3.

This enhanced sensitivity comes at the price of a smaller acceptance cone for incoming light. Therefore, an imaging sensor with microlenses may show a lower than expected sensitivity with high-aperture lenses (f -numbers smaller than 2) and show a stronger fall-off towards the edge of the array for wide-angle lenses with short focal lengths. In addition, microlenses limit **UV** sensitivity. For many applications, the advantages of microlens arrays overcome their disadvantages. They have boosted the effective *quantum efficiency* of interline transfer **CCD** sensors to 65% (Fig. 24.11a).

Color and Spectral Sensors

For color imaging, either three images sensors are required – one each for red, green, and blue – in a three-**CCD** camera, or sensor elements with different color sensitivities are used by integration of a color filter above the photosensing array and below the microlens. The most common color filter set up is the Bayer pattern. In a 2×2 pixel area, the upper left and lower right pixel have a green filter, the upper right a red, and the lower left a blue filter. Microlenses and filters make a sensor element in a solid-state imager a complex electrooptical system (Fig. 24.4).

Imaging sensors with custom color sensitivities are possible in principle, but very expensive. Thus the standard approaches either use several monochrome sensors with dichroitic beam splitters for simultaneous acquisition or a single camera with a filter wheel or a con-

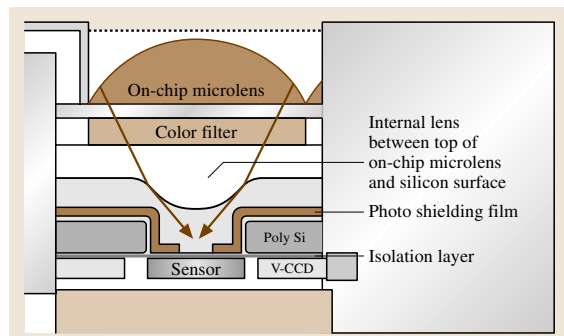


Fig. 24.4 Sketch of a sensor element of a modern **CCD** imager with a microlens and a color filter

Table 24.3 Selection of CMOS imaging sensors. C: charge saturation capacity in electrons, FR: frame rate in s^{-1} , PC: pixel clock in MHz, QE: peak quantum efficiency, HDRC: high dynamic range camera

Chip	Format $H \times V$	FR	PC	Pixel size $H \times V$ (μm)	Comments
Linear response					
Micron ^a MT9V403	656 \times 491	200	66	9.9 \times 9.9	QE 0.32 at 520 nm
Fillfactory ^b IBIS54-1300	1280 \times 1024	30	40	6.7 \times 6.7	QE 0.30–0.35 at 600 nm, C 60k
Fillfactory ^b IBIS4-4000	2496 \times 1692	4.5		11.4 \times 11.4	C 150k
Fast-frame-rate linear response					
Fillfactory ^b LUPA1300	1280 \times 1024	450	40	12.0 \times 12.0	16 parallel ports
Micron ^a MT9M440	2352 \times 1728	240	80	7.0 \times 7.0	16 parallel 10-bit ports
Micron ^{a,c} MT9M413	1280 \times 1024	600	80	12.0 \times 12.0	QE 0.27 at 520 nm, C 63k, 10 parallel 10-bit ports
Photron APX-RSd	1024 \times 1024	3000	?	17.0 \times 17.0	?
Logarithmic response					
IMS, Stuttgart HDRC ^e	640 \times 480	30	10	12.0 \times 12.0	
PhotonFocus EMPHIS-300 ^{f,g}	748 \times 480	60	20	10.6 \times 10.6	C 200k
PhotonFocus ^{f,g}	1024 \times 1024	150	80	10.6 \times 10.6	QE 0.29 at 600 nm, C 200k

^a<http://www.framos.de>, ^b<http://www.fillfactory.com>, ^c<http://www.pco.de>, ^d<http://www.photron.com>, ^e <http://www.ims-chips.de>,
^f<http://www.photonfocus.com>, ^glinear response at low light levels with adjustable transition to logarithmic response

trollable bandpass filter for consecutive acquisition of different color channels. Spectroscopic imaging or hyperspectral imaging uses a dispersive element, such as a grid or a prism, to map the wavelength onto one spatial coordinate of the sensor. In this way, however, spectral data can only be taken along one spatial coordinate. The acquisition of spectral images requires scanning in the missing spatial direction.

24.3.4 Standard Interfaces for Digital Cameras

Unfortunately, there is no unique standard available to transfer the serial stream of digital image data from a camera to a computer. Besides proprietary digital image data communication, four standard digital links are used to connect digital cameras to computers.

Camera Link

The oldest standard is the Camera Link standard. It is based on the serial communication protocol known as Channel Link and uses several such serial channels to transfer image data and control signals. Depending on the number of serial channels used in parallel (base, medium or full configuration) 24, 48 or 64 bits can be transported with clock rates of 20–60 MHz. At a clock rate of 40 MHz, this results in data rates of 120, 240, and 320 MB/s.

Camera Link is the fastest available standard. Standard personal computer (PC) bus systems such as the peripheral component interconnect (PCI) bus can only cope with the base configuration; the medium and full configuration require faster bus systems such as the recently introduced PCI express bus. This fact underlines a serious handicap of high-speed imaging. While affordable high-speed image sensors are available with serial pixel rates of more than 1000 Mpixel/s (Table 24.3), standard peripheral bus systems cannot handle these fast data streams. This problem makes high-speed imaging expensive. An intermediate storage system is required and limits the continuously recordable image sequences currently to several GB of image data.

Another big disadvantage of the Camera Link standard is that only the physical layer including the connectors are standardized. The way in which the camera is controlled, e.g., the exposure time or trigger mode, is still proprietary and requires the adaption of software drivers for each manufacturer or even camera.

Firewire and USB2

These two standards connect digital cameras to personal computers via standard bus systems, which are used for many other peripheral devices. Their advantage is their low cost. Even the power supply for the camera is provided by the bus systems. The disadvantages are the low maximum throughput of about 30–40 MBytes/s

and the short connection lengths of 5 m without bus repeaters.

While with the Firewire or IEEE1394 buses at least a standard is defined for handling the basic functionality of cameras (DCAM, <http://www.1394ta.org>), standardization does not exist at all for USB2. With the IEEE1394b extension of the Firewire standard, some disadvantages have been removed; the maximum throughput is doubled and with optical fiber connections large distances between the camera and PC can be bridged.

GigE Vision and GenICam

The latest development is the GigE Vision standard that takes advantage of the high data rates possible with gigabit Ethernet networking connections. A significant advantage of this new standard is the fact that the vision industry has finally agreed to develop a generic programming interface to handle digital cameras independent of the interface technology. Camera Link, IEEE1394 DCAM, and GigE Vision are supported by this standard (<http://www.emva.org>, <http://www.GenICam.org>).

24.4 Performance of Imaging Sensors

This section introduces the basic terms that describe the response of detectors to incident radiation. Most of these quantities characterize an individual sensor, but some also describe the nonuniformity of an array of sensors in an imaging sensor [24.4–6].

24.4.1 Responsivity

The basic quantity that describes the sensitivity of a sensor to radiation is called its *responsivity* R . The responsivity is given as the ratio between the flux Φ incident on the detector area and the resulting signal s :

$$s = R\Phi . \quad (24.1)$$

A good detector shows a constant responsivity over a wide range of radiative fluxes. A constant responsivity means that the signal is directly proportional to the incident flux. The units of responsivity are either A/W or V/W, depending on whether the signal is measured as an electrical current or voltage, respectively.

24.4.2 Quantum Efficiency

The term to describe the responsivity of a sensor is the *quantum efficiency* (QE). It relates to the particulate nature of electromagnetic radiation and the electric signal. The quantum of electromagnetic radiation, the photon, carries an energy $h\nu$, where h is Planck's constant and ν is the frequency of the radiation. The quantum of electric charge is the elementary charge e . So the quantum efficiency η is the ratio of induced elementary charges e , N_e , and the number of incident photons N_p :

$$\eta = N_e / N_p . \quad (24.2)$$

For low-energy radiation, the quantum efficiency is always lower than one for photosensors where one photon can generate at most one elementary charge. Not all incident photons generate a charge unit, because some are reflected at the sensor surface, some are absorbed in a region of the sensor where no electric charges are collected, and some are transmitted through the sensor without being absorbed. For high-energy radiation, e.g., ultraviolet (UV) and X-ray radiation absorbed in silicon, many charge units can be generated, depending on the energy of the radiation and the properties of the sensor material.

The elementary relation between the quanta for electromagnetic radiation and electric charge can be used to compute the responsivity of a detector. The radiative flux measured in photons is given by

$$\Phi_e = h\nu dN_p dt . \quad (24.3)$$

The resulting current I is given as the number of elementary charges per unit time multiplied by the elementary charge

$$I = e \frac{dN_e}{dt} , \quad (24.4)$$

and the responsivity as

$$R(\lambda) = \frac{I}{\Phi_e} = \eta(\lambda) \frac{e}{hc} \lambda \approx 0.8066 \eta(\lambda) \lambda \left[\frac{\text{A}}{\text{W}\mu\text{m}} \right] . \quad (24.5)$$

The responsivity increases linearly with wavelength, as radiation is quantized into smaller units for larger

wavelengths. Thus, a detector for infrared radiation in the 3–5 μm range is intrinsically about 10 times more sensitive than a detector for light. For practical purposes, it is important to realize that the responsivity of a detector is weakly dependent on many parameters. Among others, these include the angle of the incident light, the temperature of the detector, fatigue, and aging.

24.4.3 Signal Irradiance Relation

As illustrated in Fig. 24.1, the irradiation collected by a photosensor is finally converted into a digital number g at each sensor element of a sensor array. Thus the overall gain of the sensor element can be expressed by a single digital gain constant K that relates the number of collected charge units to the digital number g :

$$g = KN_e. \quad (24.6)$$

The digital gain constant K is dimensionless and indicates the number of digits per unit charge. An ideal charge unit counting sensor has a digital gain constant K of one.

The incident radiative flux Φ_e is received by the sensor for an exposure time t on an area A . Therefore the received radiant energy (energy-based Q_e or photon-based N_p) can be related to the irradiance incident on the sensor by

$$Q_e = \Phi_e t = A E t \quad \text{or} \quad N_p = A t \frac{\lambda}{hc} E. \quad (24.7)$$

Using (24.2) and (24.6), the relation between the incident irradiance and the digital signal g is

$$g = K \frac{A}{hc} \eta(\lambda) \lambda E(\lambda) t. \quad (24.8)$$

Normally a sensor does not receive monochromatic radiation so that (24.8) must be integrated over the spectral irradiance E_λ :

$$g = K \frac{A t}{hc} \int_{\lambda_1}^{\lambda_2} \eta(\lambda') \lambda' E_\lambda(\lambda') d\lambda'. \quad (24.9)$$

24.4.4 Dark Current

Generally, a detector generates a signal s_0 even if the incident radiative flux is zero. In a current-measuring device, this signal is called the *dark current*. A sensor

with a digital output will show a digital signal g_0 without illumination.

Thermal energy can also excite electrons into the conduction band and thus gives rise to a *dark current* even if the sensor is otherwise perfect. The probability for thermal excitation is proportional to $\exp[-\Delta E/(k_B T)]$, where ΔE is the energy difference across the band gap.

The appropriate method to limit the dark current is cooling. Because of the exponential dependency of the dark current on the absolute temperature, the dark current decreases strongly with temperature, by about a factor of two per 7–10 K. Imaging sensors cooled to liquid-nitrogen temperatures can be illuminated for hours without noticeable dark current.

24.4.5 Noise-Equivalent Exposure

The dark signal has not only a direct-current (DC) component but also a randomly fluctuating component with a standard deviation σ_0 caused by the both the statistical fluctuations of the dark current and the noise of the electronic circuits. Using the responsivity, σ_0 can be converted into an equivalent radiative flux known as the *noise-equivalent exposure* or *NEE*,

$$H_0 = \sigma_0 / R. \quad (24.10)$$

The *NEE* is related to the certain frequency band to which the detector is responding and essentially gives the minimum exposure that can be measured with a detector in that band.

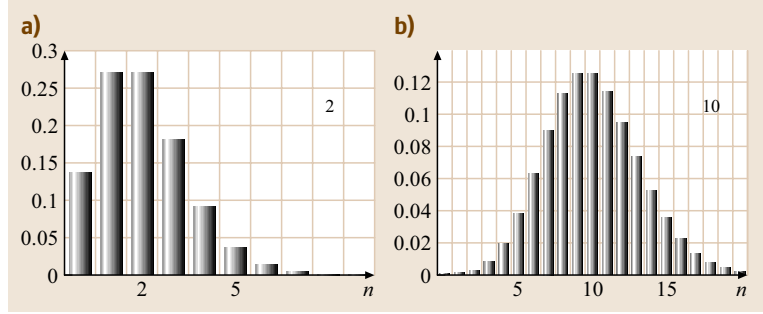
24.4.6 Saturation Equivalent Exposure

A photosensor is also limited to a maximum signal. For a digital output this is simply the largest digital number that is delivered by the analog-to-digital converter (ADC), which is $g_s = 2^D - 1$ for an ADC with D bits. As with the *NEE*, a *saturation-equivalent exposure* or *SEE* can be defined by

$$H_s = \frac{g_s}{R}. \quad (24.11)$$

There is also a physical limit for the maximum signal of a photosensor because it can only store a limited number of photoelectrons (the *full-well capacity*). This limit determines the maximum possible exposure. For an ideal sensor with a quantum efficiency of one, the maximum number of electrons is equal to the number of

Fig. 24.5 Poisson distribution (24.14) describing the counting statistics for photons for values N as indicated. With increasing \bar{n} , the distribution quickly becomes symmetrical and approaches the Gaussian distribution (24.16)



photons that can be detected in one exposure by a sensor element.

If we know the quantum efficiency and the electron capacity, it is easy to compute the saturation exposure H_s of a sensor element:

$$H_s = \eta^{-1} N_s h \nu, \quad (24.12)$$

where N_s is the full-well capacity of the sensor, and $h\nu$ is the energy of the photon. For light at the frequency of maximum sensitivity of the eye ($\nu = 5.4 \times 10^{14}$ Hz, $\lambda = 555$ nm), with an electron capacity of $N_e = 100\,000$, and a quantum efficiency of 80%, the saturation exposure is about 4×10^{-14} J. For pixels with a size of $10\,\mu\text{m} \times 10\,\mu\text{m}$, this translates into a saturation irradiance of 10^{-6} W/cm² for an exposure time of 40 ms.

24.4.7 Dynamic Range

The *dynamic range* (DR) of an image sensor is the ratio of the maximum output signal g_s to the standard deviation of the dark signal σ_0 when the sensor receives no irradiance. The dynamic range is often expressed in units of decibels (dB) as

$$\text{DR} = 20 \log \frac{g_s}{\sigma_0}. \quad (24.13)$$

A dynamic range of 60 dB thus means that the saturation signal is 1000 times larger than the standard deviation of the dark signal.

24.4.8 Photon-Noise-Limited Performance

An ideal detector would not introduce any additional noise. Even then, the detected signal is not noise-free, because the generation of photons itself is a random process. Whenever the detector related noise is below

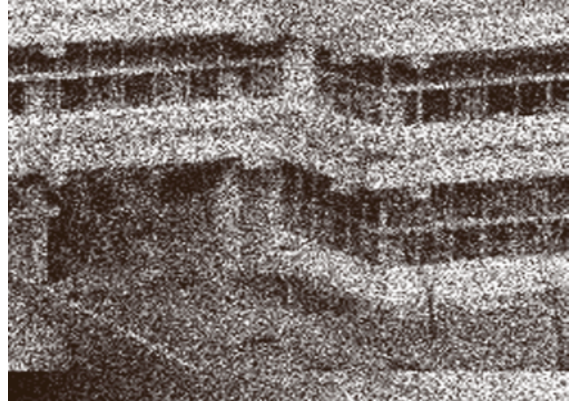


Fig. 24.6 A low-light image taken with a maximum of 10 photons

the photon noise, a detector is said to have *photon-noise-limited* performance. Photon generation is (like radioactive decay) a random process with a *Poisson distribution*. The probability density function (PDF) is given by

$$p_P(n) = \frac{N^n \exp(-N)}{n!}. \quad (24.14)$$

This equation gives the probability that n photons are detected in a certain time interval when on average N are detected. The variance of the Poisson distribution σ_n^2 ,

$$\sigma_n^2 = \sum_n p_P(n) (n - N)^2 = N, \quad (24.15)$$

is equal to the average value N .

For low mean values, the Poisson PDF is skewed with a longer tail towards higher values Fig. 24.5. However, even for moderate N , the Poisson distribution quickly converges to the continuous *Gaussian distribution* (also known as the *normal distribution*) given

by

$$p_n(x) = \exp - \frac{(x - N)^2}{2N} \quad (24.16)$$

with an equal mean value and variance. Figure 24.6 shows an example of low-light images taken with a low number of photons.

Note that, if a sensor element can store even 1 000 000 electrons, the standard deviation of the irradiance measurement is not better than 0.1%, even if the only noise source of the sensor is the photon noise. CCD sensors have an electron capacity of 10 000–500 000 electrons; only devices sensitive in the infrared range with larger sensor elements have a significantly higher capacity of up to 10 million electrons.

24.4.9 Linear Noise Model for Image Sensors

The photosignal for a single pixel is Poisson distributed as discussed in the previous section. The electronic circuits add a number of other noise sources. For practical purposes, it is however only important to know that these noise sources are normal distributed and independent of the photon noise and have a variance of σ_d . According to the laws of error propagation, the noise variances add up linearly. Therefore the noise variance of the total number of generated charge units $N = N_0 + N_e$ is given by

$$\sigma_N = \sigma_d^2 + \sigma_{N_e}^2 = \sigma_{N_0}^2 + N_e. \quad (24.17)$$

According to (24.18), the digital signal is given as

$$g = g_0 + KN. \quad (24.18)$$

An arbitrary signal g_0 is added here to account for an offset in the electronic circuits. Then the variance σ_g^2 can be described by only two terms as

$$\sigma_g^2 = K^2(\sigma_d^2 + N_e) = \sigma_0^2 + K(g - g_0). \quad (24.19)$$

The term $\sigma_0^2 = K^2\sigma_d^2$ includes the variance of all non-signal-dependent noise sources. The units of σ_d and σ_d are number of electrons (e^-) and digits (DN). Equation (24.19) predicts a linear increase of the noise variance with the measured gray value g . In addition it can be used to measure the absolute gain factor K (photon transfer method [24.4]).

24.4.10 Signal-to-Noise Ratio

The responsivity is not a good measure for a sensor, because a sensor with a high responsivity can be very noisy.

The precision of the measured irradiance rather depends on the ratio of the received signal and its standard deviation σ_g . This term is known as the *signal-to-noise ratio (SNR)*:

$$\text{SNR} = \frac{g - g_0}{\sigma_g} = \frac{g'}{\sigma_g}. \quad (24.20)$$

The inverse $\text{SNR} \sigma_g/g'$ gives the relative resolution of the irradiance measurements. A value of $\sigma_g/g' = 0.01$ means, e.g., that the standard deviation of the noise level corresponds to a relative change in the irradiance of 1%.

The discussion in the previous section has shown that the most important quantity of an image sensor is the relation of the signal quality expressed by the signal-to-noise ratio to the irradiation H . Using (24.18) and (24.19), this relation can be expressed in the simplest way by

$$\text{SNR} = \frac{N_e}{\sqrt{\sigma_d^2 + N_e}} = \frac{N_p}{\sqrt{\eta^2 \sigma_d^2 + \eta N_p}}. \quad (24.21)$$

At high irradiation ($Kg' \gg \sigma_0^2$) this equation reduces to

$$\text{SNR} = \sqrt{\frac{N_p}{\eta(\lambda)}} \quad (24.22)$$

and at low irradiation to

$$\text{SNR} = \frac{N_p}{\eta(\lambda)\sigma_d}. \quad (24.23)$$

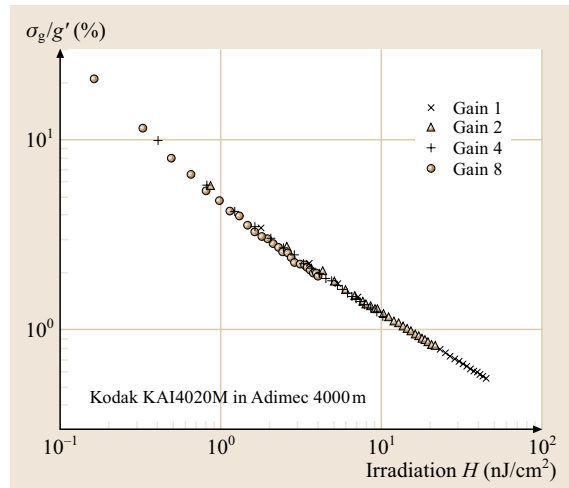


Fig. 24.7 Inverse signal-to-noise ratio σ/g' versus irradiation for an Adimec A4000m with a Kodak KAI-4020M sensor at four different gains as indicated

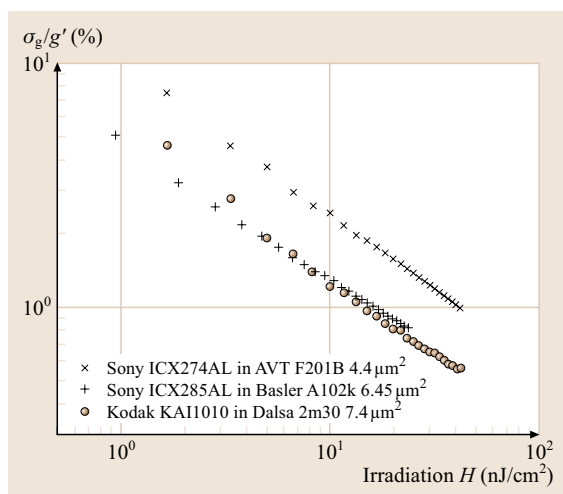


Fig. 24.8 Influence of pixel size on the relation between the inverse signal-to-noise ratio σ/g' and the irradiation

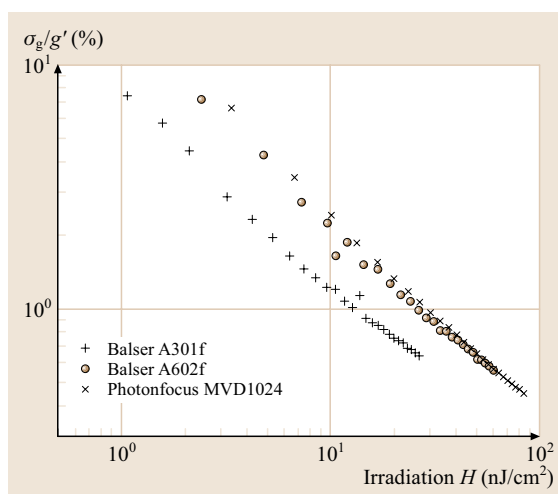


Fig. 24.10 Comparison of interline CCD (Basler A301f) and CMOS (Basler A602f, Photofocus MVD 1024) sensors with pixels of the same size

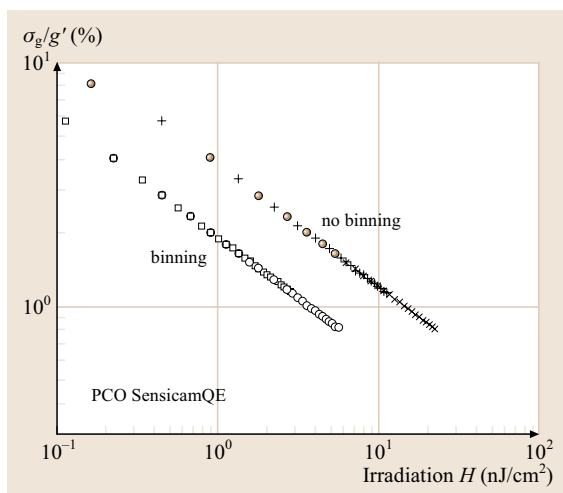


Fig. 24.9 Influence of binning on the relation between the inverse signal-to-noise ratio σ/g' and the irradiation

The number of photons perceived by a sensor element can be computed from the irradiance, area of the sensor element, and the exposure time according to (24.7).

These equations give surprisingly simple and general answers for the most important quality parameters of imaging sensors. They clearly show that the SNR increases at high irradiance levels with the square root of the quantum efficiency and the area

of the sensor element. The SNR does not depend on the amplification factor K at all. Increasing the amplification only increases the signal but not its quality.

Only recently, the European Machine Vision Association (EMVA, <http://www.emva.org/>) established the EMVA1288 standard for a comparable characterization of cameras and imaging sensors. The results of some measurements of the SNR as a function of the irradiation are discussed in the following. First, Fig. 24.7 proves that the gain does not influence the relation between the SNR and irradiation at all. At higher gain lower irradiations are reached, but at the price of a worse SNR. The values at the highest possible irradiation give the best SNR that is possible with a given camera.

Figure 24.8 demonstrates that sensors with large pixel areas generally result in a higher SNR because larger pixel have a larger full-well capacity Sect. 24.4.6.

The sensitivity of an imaging sensor can be significantly increasing by a technique called *binning* Fig. 24.9. Here the charges of pixels of a small neighborhood, e.g., a 2×2 neighborhood, are collected together. This reduces the spatial resolution in horizontal and vertical direction by a factor of two, but increases the sensitivity by a factor of four. Note that binning does not generally increase the SNR.

Finally, Fig. 24.10 compares CCD and CMOS sensors with the same pixel size. The two CMOS sensors show about two times lower sensitivity, because these two sensors do not use microlens arrays to increase the

Table 24.4 Imaging sensors for the infrared (IR), C: full-well capacity in millions of electrons [Me], IT: integration time, NETD: noise-equivalent temperature difference, QE: peak quantum efficiency

Chip	Format $H \times V$	FR	PC	Pixel size $H \times V (\mu\text{m})$	Comments
Near-infrared (NIR)					
Indigo ¹ InGaAs	320 × 256	345		30 × 30	0.9–1.68 μm , C 3.5 Me
Mid-wave infrared (MWIR)					
AIM ² PtSi	640 × 486	50	12	24 × 24	3.0–5.0 μm , NETD < 75 mK at 33 ms IT
Indigo ¹ InSb	320 × 256	345		30 × 30	2.0–5.0 μm , C 18 Me
Indigo ¹ InSb	640 × 512	100		25 × 25	2.0–5.0 μm , C 11 Me
AIM ² HgCdTe	256 × 256	800	20	40 × 40	3.0–5.0 μm , NETD < 20 mk at 1.2 ms IT, C 14 Me
AIM ² HgCdTe	384 × 288	120	20	24 × 24	3.0–5.0 μm , NETD < 20 mk at 2 ms IT
AIM ² /IaF FhG ³ QWIP	640 × 512	30	18	24 × 24	3.0–5.0 μm , NETD < 15 mk at 20 ms IT
Long-wave infrared (LWIR)					
AIM ² HgCdTe	256 × 256	200	16	40 × 40	8–10 μm , NETD < 20 mk at 0.35 ms IT
Indigo ¹ QWIP	320 × 256	345		30 × 30	8.0–9.2 μm , C 18 Me, NETD < 30 mk
AIM ² /IaF FhG ³ QWIP	256 × 256	200	16	40 × 40	8.0–9.2 μm , NETD < 8 mk at 20 ms IT
AIM ² /IaF FhG ³ QWIP	640 × 512	30	18	24 × 24	8.0–9.2 μm , NETD < 10 mk at 30 ms IT
Dual band					
AIM ² QWIP	388 × 284	100	80	40 × 40	4.8 and 8.0 μm peak, NETD < 25 mk
Uncooled sensors					
Indigo ¹ Microbolometer	320 × 240	60		30 × 30	7.0–14.0 μm , NETD < 120 mk
FLIR ¹ ThermoCAM 640	640 × 480	30		?	7.5–13.0 μm , NETD < 80 mk
Sources: ¹ http://www.flir.com , ² http://www.aim-ir.de , ³ http://www.iaf.fhg.de					

light-collecting area. However, the SNR is significantly better. This indicates that these two CMOS sensors

have a higher full-well capacity than the corresponding interline CCD sensor with the same pixel area.

24.4.11 Spectral Sensitivity

The band gap of the semiconductor material used for the detector determines the minimum energy of the photon to excite an electron into the conduction band and thus the maximum wavelength that can be detected. For silicon, the threshold given by the band gap is at about 1.1 μm . Thus, imaging detectors based on silicon are also sensitive in the near-infrared. Other materials are required to sense radiation at larger wavelengths (Table 24.1). The response for shorter wavelengths largely depends on the design. Standard imagers are sensitive down to about 350 nm. Then, the photons are absorbed in such a short distance that the generated electrons do not reach the accumulation regions in the imagers. With appropriate design techniques, however, imaging silicon sensors sensitive for ultraviolet radiation and even X-rays can be made (Table 24.1).

An ideal photodetector has a *quantum efficiency* of unity. This means that each photon irradiating the sensor generates an electron. Real devices come quite close to this ideal response. Even standard commercial devices have peak quantum efficiencies of about 0.65 (Fig. 24.11a) while scientific-grade devices may reach quantum efficiencies of up to 0.95 (Fig. 24.11b). This can be achieved by illuminating a thinned sensor from the back and by using appropriate antireflection coating. In this way it is also possible to extend the sensitivity far into the ultraviolet.

Modern CCD sensors do not show much variation in the spectral sensitivity in the visible range (Fig. 24.11). There are, however, significant differences in the ultraviolet and infrared spectral range.

The sensitivity in the ultraviolet (UV) range is generally low but there are special sensors available with enhanced UV sensitivity (Fig. 24.11). Note that the UV sensitivity is also influenced by the material used for the glass window protecting the CCD sensor. Standard CCD sensors do not use a quartz glass window and thus typically cut off the sensitivity for wavelengths below 360 nm.

All sensors are also sensitive in the near-infrared (near-IR) range, but the sensitivity does not extend beyond 1000 nm, because silicon becomes transparent at larger wavelengths. There is a general tendency for the IR sensitivity to decrease with the size of the pixels. There are special sensors available with enhanced IR sensitivity (Fig. 24.11). Many camera vendors, however, integrate an infrared cut-off filter to limit the sensitivity of the CCD sensor to the visible range.

The spectral sensitivity of CMOS sensors (Table 24.3) typically differs somewhat from that of CCD sensors. The peak sensitivity is shifted from about 550 nm to about 650 nm and the sensitivity is higher in the infrared. Thus, one cannot generally say that current CMOS sensors are less sensitive than CCD sensors. A direct comparison of the Sony ICX074AL CCD sensor with the Micron MT9V403 CMOS sensors, e.g., shows

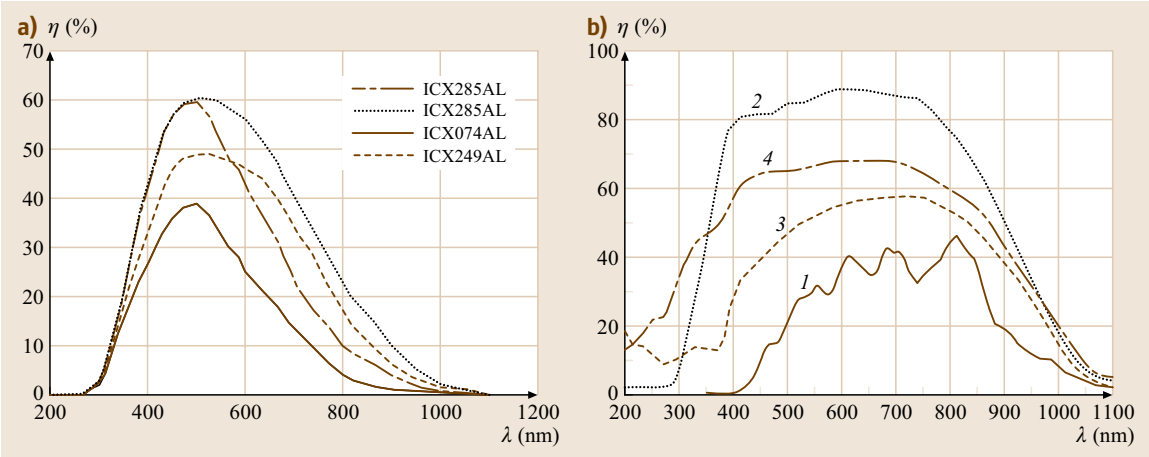


Fig. 24.11a,b Quantum efficiencies in % for (a) some commonly used Sony CCD sensors (see Table 24.2) as indicated, data courtesy of PCO AG, Kelheim, Germany. (b) Scientific-grade CCD sensors as indicated (data from Scientific Imaging Technologies, Inc. (SITE), Beaverton, Oregon)

that the **CMOS** sensor is about two times less sensitive at 550 nm but more sensitive at wavelengths larger than 750 nm.

Sensors that are sensitive in the mid (3.0–5.0 μm) and long (8.0–14.0 μm) infrared range for thermal sensing require special and expensive semiconductor materials with lower band gaps (Tables 24.1, 24.4, [24.7]). In order to limit the dark current (Sect. 24.4.4), it is also required to cool the sensors down to cryogenic temperatures (60–100 K). Only thermal detector array-based thermoconductivity (bolometer arrays) and pyroelectric sensors can be operated at room temperatures. However, these sensors are typically one order of magnitude less sensitive. The noise-equivalent temperature difference (NEDT) is only 70–100 mK, while it is 7–20 mK for quantum detectors.

24.4.12 Nonuniform Responsivity

For an imaging sensor that consists of an array of sensors, it is important to characterize the nonuniformity in the response of the individual sensors since it significantly influences the image quality. Both the dark signal and the responsivity can vary. The nonuniformity of the dark signal becomes evident when the sensor is not illuminated and is often referred to as the *fixed pattern noise* (**FPN**). This term is a misnomer. Although the nonuniformity of the dark current appears as noise, it is that part of the dark signal that does not fluctuate randomly but is a static pattern. The correct expression is *dark signal nonuniformity* (**DSNU**). When the sen-

sor is illuminated, the variation in the responsivity of the individual sensors leads to an additional component of the nonuniformity. This variation of the image sensor under constant irradiance is called the *photoresponse nonuniformity* (**PRNU**).

If the response of the image sensors is linear, the effects of the nonuniform dark signal and responsivity can be modeled with (24.1) as

$$\mathbf{G} = \mathbf{R} \cdot \mathbf{H} + \mathbf{G}_0, \quad (24.24)$$

where all terms in the equation are matrixes.

The photoresponse nonuniformity σ_R is often simply given by the standard deviation:

$$\sigma_R^2 = \frac{1}{MN-1} \sum_{m=0}^{M-1} \sum_{n=0}^{N-1} (r_{m,n} - \bar{R})^2$$

with $\bar{R} = \frac{1}{MN} \sum_{m=0}^{M-1} \sum_{n=0}^{N-1} r_{m,n}.$ (24.25)

24.4.13 Artifacts and Operation Errors

Given the complexity of modern imagers, the quality of the acquired images can seriously suffer by misadjustments or by simply operating them incorrectly. It can also happen that a vendor delivers a sensor that is not well adjusted. In this section, we therefore show some common misadjustments and discuss a number of artifacts limiting the performance of imaging sensors.

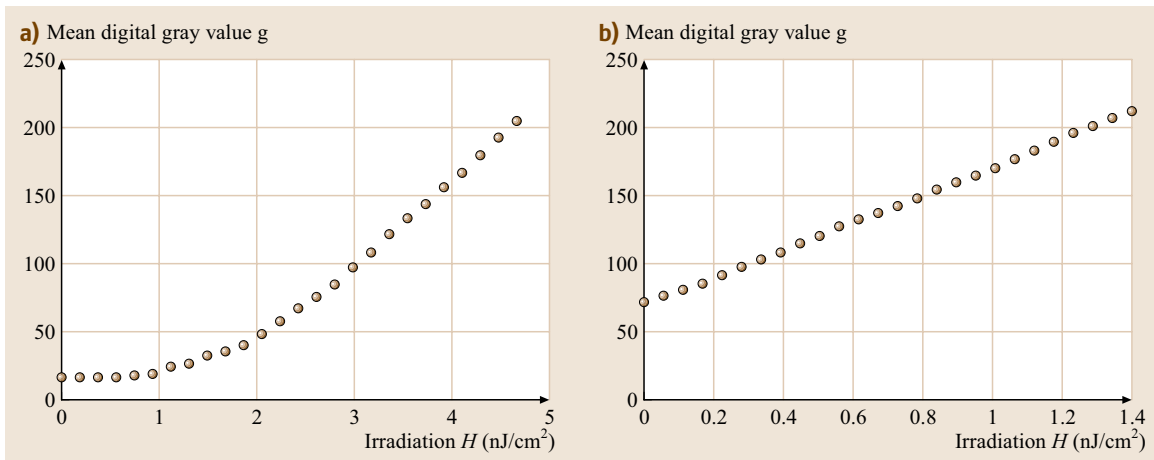


Fig. 24.12a,b Bad digital camera signals by misadjustments: (a) nonlinear response at low irradiance, (b) too high values for the dark image

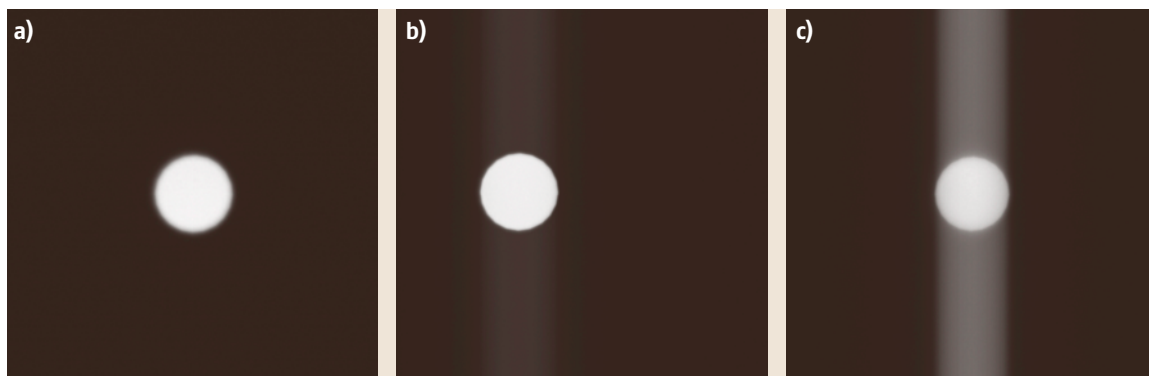


Fig. 24.13a–c Smear effects observed by constant illumination and a short exposure time of $20\ \mu\text{s}$ with (a) PCO pixelfly scientific (Sony ICX285AL sensor, diameter of spot: about 80 pixel); (b) PCO pixelfly qe (Sony ICX285AL sensor, diameter of spot: about 80 pixel); (c) Basler A602f CMOS camera (Micron MT9V403 sensor, diameter of spot: about 54 pixel)

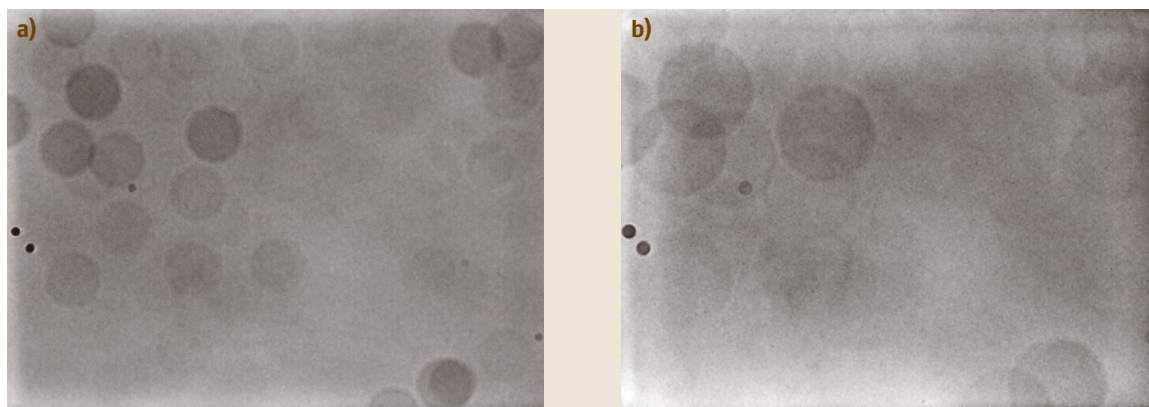


Fig. 24.14a,b Small dirt particles on the cover glass of a CCD sensor and the IR cut-off filter made visible by illuminating the sensor with uniform diverging light corresponding to an aperture of (a) 10.6, and (b) 6.1. The images are contrast enhanced with ranges that cover $\pm 2\%$ and $\pm 1\%$ change in intensity, respectively

Misadjustments

A serious misadjustment is a strong nonlinearity shown in (Fig. 24.12a). The trouble with such nonlinearity is that it can barely be detected by just observing images of the camera. In order to discover such a misadjustment, a sophisticated linearity measurement is required. It is much easier to detect and avoid too high an offset value, as shown in (Fig. 24.12b). Especially disturbing is an underflow. Then the digital gray values are zero below a critical irradiation and it appears that the dark image shows no noise.

Blooming and Smear

When short exposure times in the μs range are used with constant illumination, an artifact known as *smear*

can be observed. This effect is caused by the tiny residual light sensitivity of the interline storage areas. At exposure times equal to the read-out time, this causes no visible effects. When the exposure time is only a small fraction of the read-out time (e.g., $20\ \mu\text{s}$ versus 100 ms), additional charges are accumulated when a charge packet is transferred through an illuminated area. Therefore vertical streaks are observed when a small area is illuminated (Fig. 24.13a,b). In contrast to CCD sensors, CMOS sensors do not show smear effects (Fig. 24.13c).

Another artifact, known as *blooming*, occurs in over-exposed areas, where a part of the generated charges leaks to neighboring pixels. Modern CCD imaging sensors include antiblooming circuits so that this effect

occurs only with high overexposure. Some CMOS sensors also show blooming.

Dirt on the CCD Cover Glass

A trivial but ubiquitous flaw is dirt on the cover glass of the CCD sensor. Dirt can significantly contribute to the inhomogeneity of the sensor responsivity (PRNU, see Sect. 24.4.12). The images in Fig. 24.14 were taken by removing the lens from the camera and illuminating the chip with an integrated sphere. In this way, the dirt

is directly projected onto the chip surface. The visibility of dirt in images strongly depends on the f -number. At lower f -numbers it is less visible because the projection onto the chip is very blurred due to the more-convergent light beams.

Cleaning of the window of a CCD imager is very difficult. Therefore the first rule is to keep dirt from settling on the window by removing the cover or lens of the camera only when required and then only in a clean environment.

24.5 Camera Selection

There is no generally valid answer to the question of what is the best imaging sensor. In Sect. 24.4 we have seen that there are many different quantities that describe the quality of an imaging sensor. The demands of the application determine which of these features are the most important. In the following, a number of typical demands in applications and their implication for camera selection are discussed.

24.5.1 Measurements at Low Light Levels

Intuitively, one would argue that in this case, a camera with a high responsivity is required. What really counts, however, is the signal-to-noise ratio (SNR) at *low irradiation* levels, see (24.23). This signal-independent dark noise depends most significantly on the read-out frequency of the pixels. A higher read-out frequency requires a higher bandwidth of the electronic circuits, which implies a higher noise variance. Modern CCD sensors, such as the Sony ICX285AL (Table 24.2), show σ_d values of only a few electrons (about 4–12) even for high read-out frequencies.

Dark noise levels below one electron can only be achieved with imaging sensors that amplify the generated charge unit in some way, so-called *intensified CCD sensors* (ICCD).

The newest development in this direction are electron-multiplying circuits (EM-CCD) that are integrated as a last stage of the charge-transfer chain before the charge is converted into a voltage (Table 24.2). In this way, the charge is multiplied but not the dark noise, leading to a suppression of σ_d proportional to the charge gain factor A . The price to be paid is that the randomness of the gain multiplication introduces an excess noise factor e , which is about 1.4. Once the dark noise is low compared to the photon noise, it appears as if the quan-

tum efficiency of an EM-CCD would be $1.4^2 \approx 2$ times smaller than for a non-charge-multiplying sensor, see (24.22).

If long exposure times can be afforded, even low irradiance results in a high irradiation of the sensor. In this case the limiting factor for good image quality is a low *dark current* (Sect. 24.4.4). This requires cooling of the sensor. The Sensicam QE and Pixelfly QE cameras from PCO, for example, use the same Sony ICX285AL CCD chip. The lower dark current of the Sensicam QE, where the CCD chip is cooled down to -12°C , allows exposure times of up to 1000 s, whereas the much higher dark current of the uncooled chip degrades the image quality of the Pixelfly QE at exposure times as low as 10 s.

24.5.2 Measurements with High Irradiance Variations

Many applications are plagued by high irradiation variations. If the illumination conditions cannot be set up to avoid such large dynamic ranges, a good sensor requires not only a low σ_d but also a high *full-well capacity* so that a high *dynamic range* is the most important quality parameter Sect. 24.4.7.

24.5.3 Precise Radiometric and Geometric Measurements

If small irradiance differences or high-precision irradiance values must be measured, a high SNR is the most important parameter (Sect. 24.4.10). The SNR of the CCD and CMOS sensors included in (Table 24.2, 3) does not exceed values of 200 close to the saturation illumination. This means that the relative standard deviation of a single irradiance measurement at a single pixel is no better than 0.5%.

A critical parameter to compare irradiances measured at different pixels is the PRNU Sect. 24.4.12. For CCD sensors the standard deviation of the PRNU is typically 0.25–0.35%, for CMOS sensors it is no better than 0.5%. Therefore the PRNU does not significantly de-

grade the accuracy of irradiance measurements for single measurements. However, when either spatial or temporal averaging is performed this is no longer the case, and one must correct the PRNU by suitable calibration measurements.

References

24.1

P.W. Kruse: *Uncooled Thermal Imaging Arrays, Systems, and Applications* (SPIE, Bellingham, WA 2001)

24.2

P. Seitz: *Solid-State Image Sensing, Handbook of Computer Vision and Applications*, ed. by B. Jähne, H. Haußecker, P. Geißler (Academic, Sam Diego 1999)

24.3

T. Etoh, D. Poggemann, G. Kreider, H. Mutoh, A. Theuwissen, A. Ruckelshausen, Y. Kondo, H. Maruno, K. Takubo, H. Soya, K. Takehara, T. Okinaka, Y. Takano: An image sensor which captures

24.4

100 consecutive frames at 1 000 000 frames/s, IEEE T. Electron. Dev. **50**, 144–151 (2003)

24.5

J.R. Janesick: *Scientific Charge-Coupled Devices* (SPIE, Bellingham, WA 2001)

24.6

G. C. Holst: *CCD Arrays, Cameras, and Displays, 2nd ed.* (SPIE, Bellingham, WA 1998)

24.7

A. J. P. Theuwissen: *Solid-State Imaging with Charge-Coupled Devices* (Kluwer, Dordrecht 1995)

G. Gaussorgues: *Infrared Thermography* (Chapman Hall, London 1994)